

# Nuclear polarization of molecular hydrogen recombined on a non-metallic surface

The HERMES collaboration<sup>a</sup>

DESY, Building le/407, Notkestrasse 85, 22603 Hamburg, Germany

Received 6 October 2003 / Received in final form 15 December 2003

Published online 24 February 2004 – © EDP Sciences, Società Italiana di Fisica, Springer-Verlag 2004

**Abstract.** The nuclear polarization of H<sub>2</sub> molecules formed by recombination of nuclear polarized H atoms on the surface of a storage cell initially coated with a silicon-based polymer has been measured by using the longitudinal double-spin asymmetry in deep-inelastic positron-proton scattering. The molecules are found to have a substantial nuclear polarization, which is evidence that initially polarized atoms retain their nuclear polarization when absorbed on this type of surface.

**PACS.** 29.25.Pj Polarized and other targets – 34. Atomic and molecular collision processes and interactions – 39.10.+j Atomic and molecular beam sources and techniques – 13.88.+e Polarization in interactions and scattering

## 1 Introduction

During recent years, increased use has been made of nuclear-polarized hydrogen and deuterium gas targets, which are placed in the circulating beams of storage rings. In order to increase their thickness over that obtained by a jet of polarized atoms, the beam from atomic sources is directed into an open-ended, cooled tube (*storage cell*) in which the atoms make several hundred wall collisions before escaping. In order to maintain high polarization of the atomic gas, the storage cells are usually coated with e.g. chemically nonreactive polymers [1–3]. Examples of the successful use of this technique are measurements of spin correlation parameters in proton-proton scattering at the Indiana University Cyclotron Facility (IUCF) [5], studies of nucleon electromagnetic form factors at the storage rings VEPP-3 in Novosibirsk [6] and AmPS at NIKHEF in Amsterdam [7], and deep inelastic scattering of positrons off polarized H nuclei at the HERMES experiment situated in the HERA storage ring at DESY in Hamburg [8, 9].

A precise knowledge of the nuclear polarization of the target is required to extract interesting physics quantities from measured polarization asymmetries [5–7, 9]. At the present time, there are no convenient known scattering processes for the high-energy positrons beams available at HERA, that could provide a measure of the absolute value of the target polarization with acceptable statistics. For the HERMES experiment, therefore, a target polarimeter with good absolute precision has been con-

structed [10]. However, while the polarization of a sample of atoms from the cell is measured directly, the nuclear polarization of H<sub>2</sub> molecules which originate from recombination of hydrogen atoms in the target cell is unknown.

The nuclear polarization of recombined H<sub>2</sub> molecules was recently measured in a separate experiment at IUCF [11]. The nuclear polarization of the molecules obtained by recombination of polarized atoms on a copper surface was measured by elastic proton-proton scattering. The other existing measurement of polarization of recombined atoms concerns tensor polarized D atoms recombining on a copper surface at AmPS [12]. The absence of any measurement of the nuclear polarization of molecules recombined on a surface involving a silicon-based polymer motivated the measurement described in the present paper. The measurement was performed by comparing the double-spin asymmetries observed in deep inelastic scattering of polarized positrons from gaseous polarized hydrogen target, while the fraction of molecules was varied. The experiment was carried out using the internal target and spectrometer of the HERMES experiment at HERA. The observation of a significant nuclear polarization in the recombined molecules could be interpreted as evidence for the existence of long-lived nuclear polarization of atoms chemisorbed onto an insulating surface.

## 2 The HERMES hydrogen target

### 2.1 Set-up

A schematic diagram of the HERMES target is shown in Figure 1. A beam of nuclear-polarized hydrogen atoms is

<sup>a</sup> e-mail: lenisa@hermes.desy.de

The complete list of the authors can be found at the end of the article.

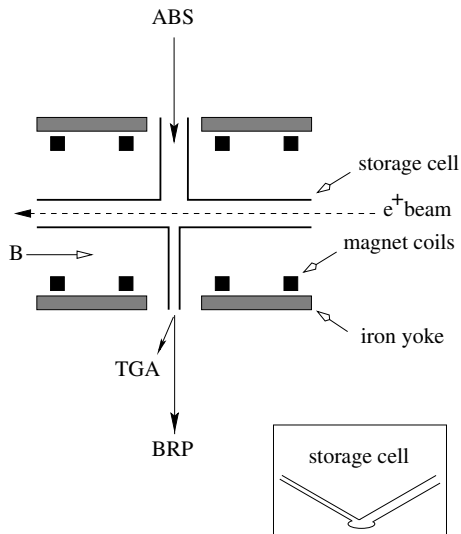


**Fig. 1.** A schematic layout of the HERMES hydrogen target. From left to right: injection tube for atomic beam source (ABS), target chamber with cell and magnet, sample tube taking gas to target gas analyzer (TGA) and Breit-Rabi polarimeter (BRP).

generated by an atomic beam source (ABS) [13] and injected into the center of the storage cell [14] via a side tube. The atoms then diffuse to the open ends of the cell where they are removed by a high speed pumping system. A magnetic field of 330 mT surrounding the cell provides a quantization axis for the spins and inhibits nuclear spin relaxation by effectively decoupling nucleon and electron spins. The atoms diffusing from a second side tube of the cell are analyzed by a Breit-Rabi polarimeter (BRP) [10] which measures the polarization of the atoms and by a target gas analyzer (TGA) [15] which determines the atomic fraction.

### 2.1.1 Cell surface

The storage cell is constructed from 99.5% pure aluminum, 75  $\mu\text{m}$  thick, it has an elliptical cross-section with 29 mm  $\times$  9.8 mm axes and a length of 400 mm. The maximum density in the cell is about  $4 \times 10^{12}$  atoms/cm<sup>3</sup>. The cell surface was initially coated with *Drifilm*, a silicon-based polymer which is radiation hard, as required in an accelerator environment [4]. The coating procedure is described in detail in reference [3]; the bake-out step of the procedure was done at 220 °C for 12 hours. The uniformity of the coating was tested visually. After coating, the cell was stored in air before being installed in the scattering chamber in HERA. The pressure in this chamber is in the  $10^{-9}/10^{-8}$  mbar range and the cell was kept at a temperature of 100 K. The storage cell is protected from the intense synchrotron radiation of the positron beam by a system of tungsten collimators upstream of the target. However, the interior surface of the target cell is intensely irradiated by positive ions that are produced in the gas by the beam and then stochastically accelerated (“heated”)

by the electric field of the very compact beam bunches as the ions spiral in the magnetic holding field until they attain an orbit large enough to reach the cell wall with energies of the order of 100 eV. Monte Carlo simulations of this process result in estimates of the dose to the cell wall surface around 10 Gy/s. After exposing the coated target cell in the proximity of the positron beam of the HERA storage ring the quality of the surface is tested again with the water-bead method [1–3], which was also used after production of the cell. It is routinely observed that the original hydrophobic Drifilm surface become hydrophilic as indicated by the changes in the wetting properties shown in this test. The measurement described in this work was carried out when the cell had been exposed to radiation for 4 months, and spanned a period of 3 weeks.

## 2.2 Target polarization

The molecules inside the HERMES target have three origins: residual gas in the scattering chamber containing the storage cell, molecules ballistically injected by the ABS and atoms that recombine after entering the cell. The hydrogen molecules present in the residual gas of the chamber originate from atoms recombining the surface of the target chamber itself, where they rapidly lose their polarization. The ballistically injected molecules were never dissociated in the beam source and therefore never polarized. For these reasons the nucleons belonging to residual gas and ballistically injected molecules are assumed to be not polarized, while the recombined molecules may have a remnant nuclear polarization.

Each contribution is directly measured with specific calibrations using the TGA as described in reference [15].

The atomic fraction  $\alpha$  is defined as:

$$\alpha = \frac{n_a}{n_a + 2n_m}, \quad (1)$$

where  $n_a$  and  $n_m$  are the atomic and molecular populations averaged over the cell. In order to distinguish unpolarized and potentially polarized molecules, the atomic fraction  $\alpha$  is separated into two factors:  $\alpha_0$  and  $\alpha_r$ ;  $\alpha_0$  defines the atomic fraction in absence of recombination, while  $\alpha_r$  defines the fraction of atoms surviving recombination in the storage cell.

The measured target polarization  $P_T$  as seen by the positron beam is described by the following expression:

$$P_T = \alpha_0 \alpha_r P_a + \alpha_0 (1 - \alpha_r) \beta P_a. \quad (2)$$

Here  $P_a$  is the nuclear polarization of the atoms in the cell. The parameter  $\beta = P_m/P_a$  represents the relative nuclear polarization of the recombined molecules with respect to the atomic polarization before recombination ( $0 \leq \beta \leq 1$ ), and it is the subject of the measurement presented in this paper.

As the particles sampled from the center of the cell have experienced a different average number of wall collisions than the ones at the ends of the cell, the properties of the measured sample are slightly different from the average values in the cell. In order to relate the average values

over the cell to the corresponding measurements on the sample beam, *sampling corrections* have to be introduced. The sampling corrections depend on the sensitivity of the BRP and the TGA to the various parts of the cell and are derived from Monte Carlo simulations of the molecular flow of gas particles traveling through the storage cell as described in reference [16]. The corrections and their uncertainties take extreme assumptions of cell surface quality into account and constitute the dominant contribution to the systematic error in the target polarization.

### 3 Measurement

#### 3.1 The HERMES spectrometer

The HERMES experiment is installed in the HERA storage ring at the DESY laboratory in Hamburg. It uses the 27.6 GeV positron beam with a typical injected current of 40 mA. The positrons are transversely polarized by emission of spin-flip synchrotron radiation [17]. Longitudinal polarization of the positron beam at the interaction point is achieved by spin rotators situated upstream and downstream of the experiment. The beam polarization is continuously measured using Compton back-scattering of circularly polarized light. Two polarimeters with low systematic uncertainties, are used, one measuring the transverse polarization in the HERA West straight section [18] and the other measuring the longitudinal polarization near the HERMES target [19]. Positron identification in the momentum range 2.1 to 27.6 GeV is accomplished by using a lead-glass calorimeter wall, a transition-radiation detector and a preshower hodoscope. This system provides positron identification with an average efficiency higher than 98% and a negligible hadron contamination. The luminosity is measured by detecting Bhabha scattered target electrons in coincidence with the scattered positrons in a pair of electromagnetic calorimeters [20]. The HERMES spectrometer is described in detail in reference [9].

#### 3.2 Method

The method adopted to extract the relative molecular polarization  $\beta$  makes use of the double spin asymmetries observed in deep-inelastic scattering of longitudinally polarized positrons off a longitudinally polarized proton target. The cross-sections  $\sigma^+$  and  $\sigma^-$  for parallel and anti-parallel relative orientations of beam and target polarizations, are related to the unpolarized cross-section  $\sigma_0$  by:

$$\sigma^{+/-} = \sigma_0(1 \mp P_B P_T A_{||}), \quad (3)$$

where  $P_B$  and  $P_T$  are the beam and target polarizations and  $A_{||}$  is the experimental double spin cross-section asymmetry. The actually measured count rate asymmetry  $C_{||}$ , however, is smaller. It is given by:

$$C_{||} = \frac{(N/L)^- - (N/L)^+}{(N/L)^- + (N/L)^+} = P_B P_T A_{||}, \quad (4)$$

**Table 1.** Atomic polarization and atomic fraction as measured at 100 K and 260 K in the HERMES storage cell, for the selected data sample.

$T_{cell}$	$P_a$	$\alpha_0$	$\alpha_r$
100 K	$0.906 \pm 0.01$	$0.96 \pm 0.03$	$0.945 \pm 0.035$
260 K	$0.939 \pm 0.015$	$0.96 \pm 0.03$	$0.26 \pm 0.04$

where  $(N/L)^{+,-}$  denotes the number of events with parallel (anti-parallel) beam and target spins orientations corrected for the background, normalized to the corresponding luminosity.

Two measurements have been performed to determine the polarization of the molecules; one with an almost purely atomic target of known polarization and a second with an enhanced molecular fraction (or smaller value of  $\alpha_r$ ). The increase in the amount of recombined molecules was achieved by increasing the temperature of the target cell from 100 K (normal running conditions) to 260 K. Over this temperature range the main mechanism thought to be responsible for recombination in the target cell is the Eley-Rideal mechanism [21] in which an atom in the gas phase hits a chemically bound atom on the surface with enough kinetic energy to overcome the activation barrier. The increase in the target temperature results in an increase of the kinetic energy of the atoms in the volume and in a higher recombination probability. No recombination happens on physically adsorbed atoms, as their coverage is negligible at 260 K. Detailed studies on various aspects of the recombination process occurring at the HERMES cell surface are reported in reference [22].

The target parameters for the two different temperatures are given in Table 1: a large increase in the fraction  $(1 - \alpha_r)$  of recombined atoms from 0.055 at 100 K to 0.74 at 260 K is observed. As the double spin asymmetry  $A_{||}$  does not depend on target or beam polarization, we can write:

$$\left( \frac{C_{||}}{P_T P_B} \right)_{100 \text{ K}} = \left( \frac{C_{||}}{P_T P_B} \right)_{260 \text{ K}}. \quad (5)$$

The target polarizations are given by (see Eq. (2)):

$$P_T^{100 \text{ K}} = \alpha_0^{100 \text{ K}} [\alpha_r^{100 \text{ K}} + (1 - \alpha_r^{100 \text{ K}})\beta^{100 \text{ K}}] P_a^{100 \text{ K}} \quad (6)$$

$$P_T^{260 \text{ K}} = \alpha_0^{260 \text{ K}} [\alpha_r^{260 \text{ K}} + (1 - \alpha_r^{260 \text{ K}})\beta^{260 \text{ K}}] P_a^{260 \text{ K}}. \quad (7)$$

The values for  $\alpha_0^{100 \text{ K}, 260 \text{ K}}$ ,  $\alpha_r^{100 \text{ K}, 260 \text{ K}}$ ,  $P_a^{100 \text{ K}, 260 \text{ K}}$  are reported in Table 1.

#### 3.3 Extraction of the parameter $\beta$

In order to extract information on  $\beta$ , a minimization procedure has been used. Equation (5) has two unknowns:  $\beta^{100 \text{ K}}$  and  $\beta^{260 \text{ K}}$ , which are independent since

the surface conditions at 100 K and 260 K are assumed to be different. The value  $\beta^{260\text{ K}}$  has been determined by varying its value until the function  $\chi^2(\beta^{260\text{ K}})$  described by:

$$\chi^2(\beta^{260\text{ K}}) = \sum_i \left[ \frac{\left( \frac{C_{||i}}{P_B P_T} \right)_{260\text{ K}} - \left( \frac{C_{||i}}{P_B P_T} \right)_{100\text{ K}}}{\left( \left( \frac{\delta C_{||i}}{P_B P_T} \right)_{260\text{ K}}^2 + \left( \frac{\delta C_{||i}}{P_B P_T} \right)_{100\text{ K}}^2 \right)^{1/2}} \right]^2 \quad (8)$$

was minimized. The minimization has been studied as a function of the parameter  $\beta^{100\text{ K}}$ . In equation (8)  $C_{||i}$  is the count rate asymmetry in the  $i$ th-bin of the kinematic plane and  $\delta C_{||i}$  is its associated statistical uncertainty. (The statistical uncertainties of  $P_T$  and  $P_B$  are negligible here.) The summation is made over all the kinematic bins of the asymmetry measurement. The binning of the kinematic plane is the same as the one adopted in the extraction of the  $g_1^p$  spin-dependent structure function of the proton from the  $A_{||}$  asymmetry, as described in [23]. It was verified, by solving equation (5) for all bins separately, that  $\beta$  does not depend on the bin number and therefore equation (8) gives the best possible result.

As at 100 K only a few percent of the gas is in molecular form ( $1 - \alpha_r = 0.055$ , as can be seen from Tab. 1), the final result is insensitive to the value assumed for  $\beta^{100\text{ K}}$ . Using the conservative assumption  $0 \leq \beta^{100\text{ K}} \leq 1$ , the following value has been obtained for  $\beta^{260\text{ K}}$ :

$$\beta^{260\text{ K}} = 0.68 \pm 0.09_{stat} \pm 0.06_{syst}. \quad (9)$$

The uncertainty of the measurement is dominated by the low statistics of the data taken at 260 K (0.19 million events) compared to the 100 K data sample (2.5 million events). The statistical uncertainty corresponds to the change in the value of  $\chi^2(\beta^{260\text{ K}})$  by one unit from its minimum, and was found to be independent of the value of  $\beta^{100\text{ K}}$ . The main source of the systematic uncertainty arises from the knowledge of  $\alpha_r^{260\text{ K}}$ . Unfortunately, the sampling corrections described in Section 2.2 cannot be applied at 260 K as the associated systematic uncertainty grows rapidly if  $\alpha_r$  is significantly below unity. Hence, an alternative method has been used to correct for this effect. Coincident Bhabha-scattering event rates measured by the luminosity monitor are proportional to the target density, which depends on the atomic fraction. (The molecules have an average velocity lower by a factor  $\sqrt{2}$ .) The comparison of the Bhabha rates detected at 100 K and 260 K with constant atomic flux injected in the cell allows one to limit the interval of  $\alpha_r^{260\text{ K}}$  to the range reported in Table 1. Some systematic uncertainties, such as those in  $\alpha_0$  and  $P_B$ , are common to both the 100 K and the 260 K measurements and cancel in the ratio in equation (8).

In Figure 2 the result of the present studies on the nuclear polarization of recombined H molecules are compared to previous measurements. In each case a non-zero nuclear polarization is observed, but the different surface conditions used in each experiment preclude a more quantitative comparison of the values themselves. Nevertheless,

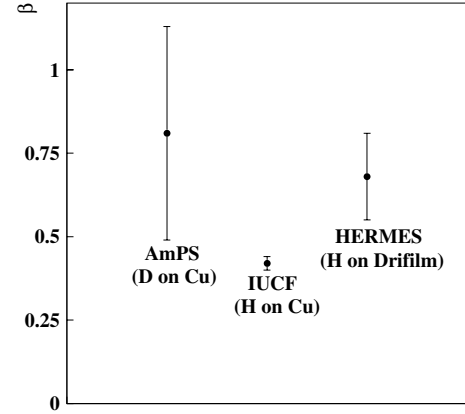


**Fig. 2.** Summary of the existing measurements of the nuclear polarization of recombined molecules. The newly obtained HERMES measurement at 260 K with a holding field of 330 mT is compared to the measurement by AmPS and IUCF obtained at room temperature and magnetic holding fields of 28 mT and 440 mT respectively.

in the discussion which follows, an explanation of these differences in terms of the variation in the properties of the surfaces has been attempted.

## 4 Discussion

### 4.1 Nuclear polarization of surface atoms

By assuming that the nucleon spins are not affected by the recombination process, the nuclear polarization of the molecule at its formation ( $P_m^0$ ) can be evaluated by taking the average value of the polarization of an atom coming from the volume ( $P_a$ ) and one resident on the surface ( $P_s$ ):

$$P_m^0 = \frac{P_a + P_s}{2}. \quad (10)$$

The loss of polarization of the molecule after recombination has been described in reference [11]. In free flight, the internal molecular fields  $B_c$  from the spin-rotation interaction and the direct dipole-dipole interaction cause the nuclei to rapidly precess around a direction which is skew to the external field by  $B_c/B$ . The orientation of  $B_c$  is randomized at each wall collision. Between successive wall collisions, the component of the polarization along the external field decreases by an amount  $(B_c/B)^2$  and after  $n$  wall bounces:

$$P_m = P_m^0 e^{-n(B_c/B)^2}, \quad (11)$$

where  $B_c$  for  $H_2$  is 6.1 mT [11]. For the HERMES cell, we have the value  $B \approx 330$  mT. Moreover, it has been estimated [16] that the number of wall collisions is of the order of 300. Hence, using equation (11), it follows that  $P_m \approx 0.9P_m^0$ . By taking the extracted value of  $\beta^{260\text{ K}}$  and the measured value of  $P_a^{260\text{ K}}$  from Table 1, we are able to give an estimate for the polarization of the atoms on the surface making use of equation (10):

$$P_s^{260\text{ K}} = 0.46 \pm 0.22_{tot}. \quad (12)$$

The total uncertainty results from adding the statistical and systematic uncertainties in quadrature. This non-zero result provides evidence that chemically bound surface atoms appear to retain some nuclear polarization.

## 4.2 Relaxation and dwell times

The present result differs from that of the experiment described in reference [11], where the measured value of  $\beta$  lower than 0.5 is compatible with a zero residual polarization of the atoms on a copper surface. As both measurements are sensitive to the nuclear polarization of the molecular gas coming from the recombination process and one atom of each recombined molecule comes from the surface, they actually compare the nuclear spin relaxation time  $\tau_r$  of atoms on the surface with the dwell time  $\tau_d$  that the atoms reside on the surface. These times are related by the equation<sup>1</sup>:

$$P_s = P_a \frac{\tau_r}{\tau_d + \tau_r}. \quad (13)$$

By using the result of reference [11] and those presented in the previous section, it is concluded that  $\tau_r \approx \tau_d$  for the HERMES cell surface and  $\tau_r \ll \tau_d$  for the copper surface, suggesting that, as expected, on a bare metal surface the relaxation processes are much stronger than on an inert surface like silane.

An upper limit for the dwell time  $\tau_d$  can be derived by considering a uniform surface where all sites are recombining and by using the inequality:

$$\tau_d < \frac{N_s}{N_{inj}(1 - \alpha_r)}, \quad (14)$$

where  $N_s$  is the total number of catalytic sites on the cell surface  $S$  and  $N_{inj}$  is the number of injected atoms per second. By assuming an area per surface site of  $4 \text{ \AA}^2$ , taking  $S \approx 0.026 \text{ m}^2$  [14],  $N_{inj} \approx 6.5 \times 10^{16}$  atoms/s [13] and  $\alpha_r \approx 0.26$  (Tab. 1) one obtains  $\tau_d \lesssim 14$  s and a similar limit for the relaxation time  $\tau_r$ .

## 5 Conclusions

In summary, the longitudinal double spin asymmetry in deep-inelastic positron-proton scattering has been used to measure for the first time the nuclear polarization of the molecules produced by recombination of hydrogen atoms on a storage cell initially prepared with Drifilm coating. The measurement shows that the molecules emerging from recombination on this surface retain a large degree of polarization. In absence of a polarizing mechanism after leav-

ing the wall, significant polarization can be inferred for the atoms on the wall. The application of a simple model allowed to derive an estimate for the depolarization time of the atoms on the surface.

The present finding of a non-negligible nuclear polarization retained by the atoms on a surface prepared with Drifilm is encouraging in view of hopes for the developing of a nuclear polarized gaseous molecular target.

We gratefully acknowledge the DESY management for its support and the DESY staff and the staff of the collaborating institutions. This work was supported by the FWO-Flanders, Belgium; the INTAS contribution from the European Commission; the European Commission IHP program under contract HPRN-CT-2000-00130; the German Bundesministerium für Bildung und Forschung (BMBF); the Italian Istituto Nazionale di Fisica Nucleare (INFN); Monbusho International Scientific Research Program, JSPS, and Toray Science Foundation of Japan; the Dutch Foundation for Fundamenteel Onderzoek der Materie (FOM); the U.K. Particle Physics and Astronomy Research Council and Engineering and Physical Sciences Research Council; and the U.S. Department of Energy and National Science Foundation.

## References

1. G.E. Thomas et al., Nucl. Instrum. Meth. A **257**, 32 (1987)
2. D.R. Swenson, L.W. Anderson, Nucl. Instrum. Meth. B **29**, 627 (1988)
3. J.A. Fedchak et al., Nucl. Instrum. Meth. A **391**, 405 (1997)
4. R. Gilman et al., Nucl. Instrum. Meth. A **327**, 277 (1993)
5. W. Haeberli et al., Phys. Rev. C **55**, 597 (1997)
6. R. Gilmann et al., Phys. Rev. Lett. **65**, 1733 (1990)
7. M. Ferro-Luzzi et al., Phys. Rev. Lett. **77**, 2630 (1996)
8. HERMES Technical Design Report, DESY-PRC 93/06, 1993
9. K. Ackerstaff et al., Nucl. Instrum. Meth. A **417**, 230 (1998)
10. C. Baumgarten et al., Nucl. Instrum. Meth. A **482**, 606 (2002)
11. T. Wise et al., Phys. Rev. Lett. **87**, 042701 (2001)
12. J.F.J. van den Brand et al., Phys. Rev. Lett. **78**, 1235 (1997)
13. A. Nass et al., Nucl. Instrum. Meth. A **505**, 633 (2003)
14. C. Baumgarten et al., Nucl. Instrum. Meth. A **496**, 277 (2003)
15. C. Baumgarten et al., Nucl. Instrum. Meth. A **508**, 268 (2003)
16. C. Baumgarten et al., Eur. Phys. J. D **18**, 37 (2002)
17. A.A. Sokolov, I.M. Ternov, Sov. Phys. **8**, 1203 (1964)
18. D.P. Barber et al., Phys. Lett. B **343**, 436 (1995)
19. M. Beckmann et al., Nucl. Instrum. Meth. A **479**, 334 (2002)
20. Th. Benisch et al., Nucl. Instrum. Meth. A **471**, 314 (2001)
21. S. Holloway, Surf. Sci. **299/300**, 656 (1994)
22. C. Baumgarten et al., Nucl. Instrum. Meth. A **496**, 263 (2003)
23. A. Airapetian et al., Phys. Lett. B **442**, 484 (1998)

<sup>1</sup> The expression has been determined by assuming the atomic polarization of the surface atoms to decay exponentially with a characteristic time  $\tau_r$  and integrating over an exponential distribution for the dwell times with characteristic time  $\tau_d$ .

## The HERMES collaboration authors

A. Airapetian<sup>30</sup>, N. Akopov<sup>30</sup>, Z. Akopov<sup>30</sup>, M. Amarian<sup>6,30</sup>, V.V. Ammosov<sup>22</sup>, A. Andrus<sup>15</sup>, E.C. Aschenauer<sup>6</sup>, W. Augustyniak<sup>29</sup>, R. Avakian<sup>30</sup>, A. Avetissian<sup>30</sup>, E. Avetissian<sup>10</sup>, P. Bailey<sup>15</sup>, V. Baturin<sup>21</sup>, C. Baumgarten<sup>19</sup>, M. Beckmann<sup>5</sup>, S. Belostotski<sup>21</sup>, S. Bernreuther<sup>8</sup>, N. Bianchi<sup>10</sup>, H.P. Blok<sup>20,28</sup>, H. Böttcher<sup>6</sup>, A. Borissov<sup>17</sup>, A. Borysenko<sup>10</sup>, M. Bouwhuis<sup>15</sup>, J. Brack<sup>4</sup>, A. Brüll<sup>16</sup>, V. Bryzgalov<sup>22</sup>, G.P. Capitani<sup>10</sup>, H.C. Chiang<sup>15</sup>, G. Ciullo<sup>9</sup>, M. Contalbrigo<sup>9</sup>, G. Court<sup>32</sup>, P.F. Dalpiaz<sup>9</sup>, R. De Leo<sup>3</sup>, L. De Nardo<sup>1</sup>, E. De Sanctis<sup>10</sup>, E. Devitsin<sup>18</sup>, P. Di Nezza<sup>10</sup>, M. Düren<sup>13</sup>, M. Ehrenfried<sup>8</sup>, A. Elalaoui-Moulay<sup>2</sup>, G. Elbakian<sup>30</sup>, F. Ellinghaus<sup>6</sup>, U. Elschenbroich<sup>12</sup>, J. Ely<sup>4</sup>, R. Fabbri<sup>9</sup>, A. Fantoni<sup>10</sup>, A. Fechtchenko<sup>7</sup>, L. Felawka<sup>26</sup>, B. Fox<sup>4</sup>, J. Franz<sup>11</sup>, S. Frullani<sup>24</sup>, G. Gapienko<sup>22</sup>, V. Gapienko<sup>22</sup>, F. Garibaldi<sup>24</sup>, K. Garrow<sup>1,25</sup>, E. Garutti<sup>20</sup>, D. Gaskell<sup>4</sup>, G. Gavrilov<sup>5,26</sup>, V. Gharibyan<sup>30</sup>, G. Graw<sup>19</sup>, O. Grebeniuk<sup>21</sup>, L.G. Greeniaus<sup>1,26</sup>, I.M. Gregor<sup>6</sup>, W. Haerberli<sup>31</sup>, K. Hafidi<sup>2</sup>, M. Hartig<sup>26</sup>, D. Hasch<sup>10</sup>, D. Heesbeen<sup>20</sup>, M. Henoch<sup>8</sup>, R. Hertenberger<sup>19</sup>, W.H.A. Hesselink<sup>20,28</sup>, A. Hillenbrand<sup>8</sup>, M. Hoek<sup>13</sup>, Y. Holler<sup>5</sup>, B. Hommez<sup>12</sup>, G. Iarygin<sup>7</sup>, A. Ivanilov<sup>22</sup>, A. Izotov<sup>21</sup>, H.E. Jackson<sup>2</sup>, A. Jgoun<sup>21</sup>, R. Kaiser<sup>14</sup>, E. Kinney<sup>4</sup>, A. Kisselev<sup>21</sup>, H. Kolster<sup>19,28</sup>, K. Königsmann<sup>11</sup>, M. Kopytin<sup>6</sup>, V. Korotkov<sup>6</sup>, V. Kozlov<sup>18</sup>, B. Krauss<sup>8</sup>, V.G. Krivokhijine<sup>7</sup>, L. Lagamba<sup>3</sup>, L. Lapikás<sup>20</sup>, A. Laziev<sup>20,28</sup>, P. Lenisa<sup>9</sup>, P. Liebing<sup>6</sup>, L.A. Linden-Levy<sup>15</sup>, K. Lipka<sup>6</sup>, W. Lorenzon<sup>17</sup>, J. Lu<sup>26</sup>, B. Maiheu<sup>12</sup>, N.C.R. Makins<sup>15</sup>, B. Marianski<sup>29</sup>, H. Marukyan<sup>30</sup>, F. Masoli<sup>9</sup>, V. Mexner<sup>20</sup>, N. Meyners<sup>5</sup>, O. Mikloukho<sup>21</sup>, C.A. Miller<sup>1,26</sup>, Y. Miyachi<sup>27</sup>, V. Muccifora<sup>10</sup>, A. Nagaitsev<sup>7</sup>, E. Nappi<sup>3</sup>, Y. Naryshkin<sup>21</sup>, A. Nass<sup>8</sup>, M. Negodaev<sup>6</sup>, W.-D. Nowak<sup>6</sup>, K. Oganessyan<sup>5,10</sup>, H. Ohsuga<sup>27</sup>, N. Pickert<sup>8</sup>, S. Potashov<sup>18</sup>, D.H. Potterveld<sup>2</sup>, M. Raithel<sup>8</sup>, D. Reggiani<sup>9</sup>, P.E. Reimer<sup>2</sup>, A. Reischl<sup>20</sup>, A.R. Reolon<sup>10</sup>, C. Riedl<sup>8</sup>, K. Rith<sup>8</sup>, G. Rosner<sup>14</sup>, A. Rostomyan<sup>30</sup>, L. Rubacek<sup>13</sup>, J. Rubin<sup>15</sup>, D. Ryckbosch<sup>12</sup>, Y. Salomatina<sup>22</sup>, I. Sanjiev<sup>2,21</sup>, I. Savin<sup>7</sup>, C. Scarlett<sup>17</sup>, C. Schill<sup>10,11</sup>, G. Schnell<sup>6</sup>, K.P. Schüller<sup>5</sup>, A. Schwind<sup>6</sup>, J. Seele<sup>15</sup>, R. Seidl<sup>8</sup>, B. Seitz<sup>13</sup>, R. Shandize<sup>8</sup>, C. Shearer<sup>14</sup>, T.-A. Shibata<sup>27</sup>, V. Shutov<sup>7</sup>, M.C. Simani<sup>20,28</sup>, K. Sinram<sup>5</sup>, M. Stancari<sup>9</sup>, M. Statera<sup>9</sup>, E. Steffens<sup>8</sup>, J.J.M. Steijger<sup>20</sup>, H. Stenzel<sup>13</sup>, J. Stewart<sup>6</sup>, U. Stösslein<sup>4</sup>, P. Tait<sup>8</sup>, H. Tanaka<sup>27</sup>, S. Taroian<sup>30</sup>, B. Tchuiko<sup>22</sup>, A. Terkulov<sup>18</sup>, A. Tkabladze<sup>12</sup>, A. Trzcinski<sup>29</sup>, M. Tytgat<sup>12</sup>, A. Vandenbroucke<sup>12</sup>, P. van der Nat<sup>20,28</sup>, G. van der Steenhoven<sup>20</sup>, M.C. Vetterli<sup>1,25,26</sup>, V. Vikhrov<sup>21</sup>, M.G. Vincter<sup>1</sup>, C. Vogel<sup>8</sup>, M. Vogt<sup>8</sup>, J. Volmer<sup>6</sup>, C. Weiskopf<sup>8</sup>, J. Wendland<sup>25,26</sup>, J. Wilbert<sup>8</sup>, T. Wise<sup>31</sup>, G. Ybeles Smit<sup>28</sup>, B. Zihlmann<sup>20</sup>, H. Zohrabian<sup>30</sup>, and P. Zupranski<sup>29</sup>

<sup>1</sup> Department of Physics, University of Alberta, Edmonton, Alberta T6G 2J1, Canada

<sup>2</sup> Physics Division, Argonne National Laboratory, Argonne, Illinois 60439-4843, USA

<sup>3</sup> Istituto Nazionale di Fisica Nucleare, Sezione di Bari, 70124 Bari, Italy

<sup>4</sup> Nuclear Physics Laboratory, University of Colorado, Boulder, Colorado 80309-0446, USA

<sup>5</sup> DESY, Deutsches Elektronen-Synchrotron, 22603 Hamburg, Germany

<sup>6</sup> DESY Zeuthen, 15738 Zeuthen, Germany

<sup>7</sup> Joint Institute for Nuclear Research, 141980 Dubna, Russia

<sup>8</sup> Physikalisches Institut, Universität Erlangen-Nürnberg, 91058 Erlangen, Germany

<sup>9</sup> Istituto Nazionale di Fisica Nucleare, Sezione di Ferrara and Dipartimento di Fisica, Università di Ferrara, 44100 Ferrara, Italy

<sup>10</sup> Istituto Nazionale di Fisica Nucleare, Laboratori Nazionali di Frascati, 00044 Frascati, Italy

<sup>11</sup> Fakultät für Physik, Universität Freiburg, 79104 Freiburg, Germany

<sup>12</sup> Department of Subatomic and Radiation Physics, University of Gent, 9000 Gent, Belgium

<sup>13</sup> Physikalisches Institut, Universität Gießen, 35392 Gießen, Germany

<sup>14</sup> Department of Physics and Astronomy, University of Glasgow, Glasgow G12 8QQ, United Kingdom

<sup>15</sup> Department of Physics, University of Illinois, Urbana, Illinois 61801-3080, USA

<sup>16</sup> Laboratory for Nuclear Science, Massachusetts Institute of Technology, Cambridge, Massachusetts 02139, USA

<sup>17</sup> Randall Laboratory of Physics, University of Michigan, Ann Arbor, Michigan 48109-1120, USA

<sup>18</sup> Lebedev Physical Institute, 117924 Moscow, Russia

<sup>19</sup> Sektion Physik, Universität München, 85748 Garching, Germany

<sup>20</sup> Nationaal Instituut voor Kernfysica en Hoge-Energiefysica (NIKHEF), 1009 DB Amsterdam, The Netherlands

<sup>21</sup> Petersburg Nuclear Physics Institute, St. Petersburg, Gatchina, 188350 Russia

<sup>22</sup> Institute for High Energy Physics, Protvino, Moscow region, 142281 Russia

<sup>23</sup> Institut für Theoretische Physik, Universität Regensburg, 93040 Regensburg, Germany

<sup>24</sup> Istituto Nazionale di Fisica Nucleare, Sezione Roma 1, Gruppo Sanità and Physics Laboratory, Istituto Superiore di Sanità, 00161 Roma, Italy

<sup>25</sup> Department of Physics, Simon Fraser University, Burnaby, British Columbia V5A 1S6, Canada

<sup>26</sup> TRIUMF, Vancouver, British Columbia V6T 2A3, Canada

<sup>27</sup> Department of Physics, Tokyo Institute of Technology, Tokyo 152, Japan

<sup>28</sup> Department of Physics and Astronomy, Vrije Universiteit, 1081 HV Amsterdam, The Netherlands

<sup>29</sup> Andrzej Soltan Institute for Nuclear Studies, 00-689 Warsaw, Poland

<sup>30</sup> Yerevan Physics Institute, 375036 Yerevan, Armenia

<sup>31</sup> Department of Physics, University of Wisconsin-Madison, Madison, Wisconsin 53706, USA

<sup>32</sup> Physics Department, University of Liverpool, Liverpool L69 7ZE, United Kingdom